NEW MAGNETIC EINZEL LENS AND ITS BEAM OPTICAL FEATURES

M.H. Rashid# and C. Mallik, VECC, Kolkata, India

Abstract

Magnetic cylindrical lens is used mostly in beam lines to focus and transport low energy beam. It is well known that focusing power of a magnetic solenoid lens depends on the ratio of particle momentum and electric charge. A solenoid rotates also an ion beam while focusing it and the phase space areas of the beam in x- and y-plane get entangled and increased. The paper reported here describes an effort to design a new magnetic einzel lens (MEL) using a pair of Glaser solenoid lens (GSL) in anti-solenoid mode for the first time to get zero rotation of the exit beam. Analytical formulae have been generated to deduce the scalar magnetic potential and field along the central axis of the lens. Thereafter, beam optics and particle tracking is done using the combined field of a pair of GSL's constituting the MEL. The required focusing power of the designed lens is achieved for a beam of given rigidity.

INTRODUCTION

We know that an electrostatic einzel lens consists of three co-axial cylinders. The mid-cylinder is kept at some potential which can be varied while the end-cylinders at small gaps are kept at constant zero potential. This creates opposite fields at the two gaps giving accelerating and decelerating force on a charged particle beam passing through the gaps along the central axis. So, the overall energy gained by the beam is zero. The focusing and defocusing effects at the gaps due to the opposite radial components of the electric field give overall focusing to the beam, which depends on the energy of the beam also.

Two iron yoked solenoids create opposing magnetic field along the central axis if they are energized oppositely and equally. They resemble electrostatic einzel lens and so we call them MEL. One solenoid rotates the beam in one direction about the central axis while the other in the opposite direction. So the overall rotation of the beam is negligible and there is almost no coupling of the sub-phase spaces in the horizontal and vertical plane resulting null growth of the phase space area. But the radial component of the magnetic field at the rising and falling regions of the field give overall focusing to the beam, which depends on the momentum of the beam.

Earlier, properties of small such lens were studied for application in electron microscope to produce small rotation-less electron beam spot with little lens aberrations. General theory of MEL was studied by Baba and Kanaya [1]. We will use more simplified model of potential and field. It is easier to construct a solenoid to confirm the axial field distribution. The particles and beam are simulated for transportation to study its beam optical features.

#E-mail: haroon@veccal.ernet.in

MAGNETIC POTENTIAL AND FIELD

The sketch of the MEL formed from two GSL; kept attached or at small gap 2G, along the beam line and energized oppositely, is shown in Fig. 1. The hatched area is the iron yoke confirms the bell shaped field for the Glaser solenoid magnet. The diameter D and pole-to-pole distance S are given for the structure of the GSL. These parameters together with the magneto-motive force (NI) set the design of Glaser lens for certain focal lengths individually for a beam of given rigidity. Design and test of Glaser type of solenoid magnet have been presented in InPAC-2009 [2]. If O is the origin, the centre of the two solenoids are at d=(S/2+G) from the origin.

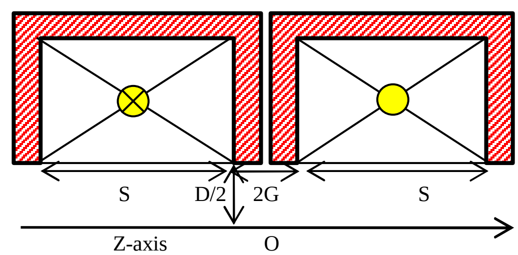

Figure 1: Cylindrically symmetric MEL in which electric current flows into and out of the page in the right and left solenoids respectively.

Magnetic Potential

The magnetic scalar potentials φ_i for a GSL are defined by eqs. (1), (2) and (3) in ref. [2] where subscript i stands for 1, 2 and 3. The forms of scalar potentials along the axis represented by φ_1, φ_2 and φ_3, which depend on the geometry of solenoid that is the pole to pole gap S and diameter D and magneto-motive force (MMF) and were expressed in detail therein.

Magnetic Field

The potential formulae for the magnetic Glaser lens are used to evaluate the field analytically. The net axial field $\varphi_i'(z)$ for a GSL is given in eqs. (1), (2) and (3) below using $\varphi_i'(z) = -\mu_0 d\varphi_i(z)/dz$. Now the magnetic field for a MEL as depicted in Fig. 1 is given by eq. (4) using the three fields from three potentials for i = 1, 2 and 3. The evaluated fields of the MEL for S=10 cm, D=10 cm, G= 0 cm, 5 cm, 10 cm and NI=37000 A-turn are shown in Figs. 2a and 2b. The GSL field is given by eq. (1) in ref. [3].

$$\varphi_1'(z) = \frac{-\mu_0 NI}{\pi S}\int_0^{\infty} \frac{2\sin(Sx/D)\cdot\cos(2xz/D)}{x\cdot I_0(x)}dx \quad (1)$$

Where $I_0(x)$ is the modified Bessel function of first kind and order zero. The integration is in radial direction using the dummy variable x. Another field form is given by eq. (2) below.

$$\varphi_2'(z) = \frac{-\mu_0 NI}{\pi S}(P - Q) \tag{2}$$

$$P = \frac{z_+}{1 + z_+^2} + \tan^{-1}(z_+) \tag{2a}$$

$$Q = \frac{z_-}{1 + z_-^2} + \tan^{-1}(z_-) \tag{2b}$$

Where, $z_+ = (2z + S)/D$, $z_- = (2z - S)/D$, it is deduced from electric scalar potential form given by Szilagyi [4] for two apertures at the two solenoid pole ends. Complete and closed optical analysis of GSL is done by eq. (3).

$$\varphi_3'(z) = \frac{-\mu_0 NI}{b}\left(\frac{1}{1 + (z/a)^2}\right) \tag{3}$$

Where, $b=\sqrt{(S^2+0.45D^2)}$ and $a=0.485b$ are the semi-empirical expressions to adjust the bell-shaped field due to an iron shielded solenoids and they are popularly known as Glaser model as the lens problem with this field configuration was solved by Glaser in [3, ch.VII] and [5].

$$B_i(z) = \varphi_i'(z - d) - \varphi_i'(z + d) \tag{4}$$

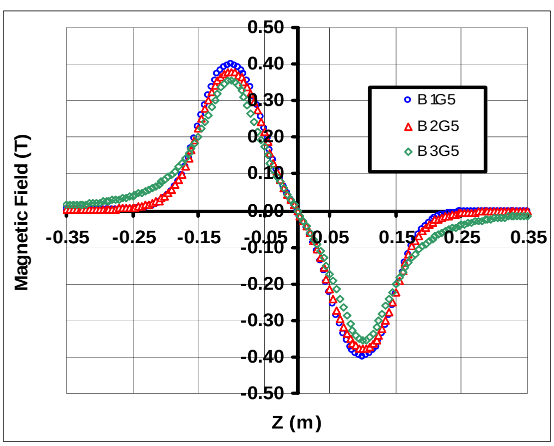

Figure 2a: Magnetic field B1 to B3 calculated from corresponding potential forms at gap G=5cm.

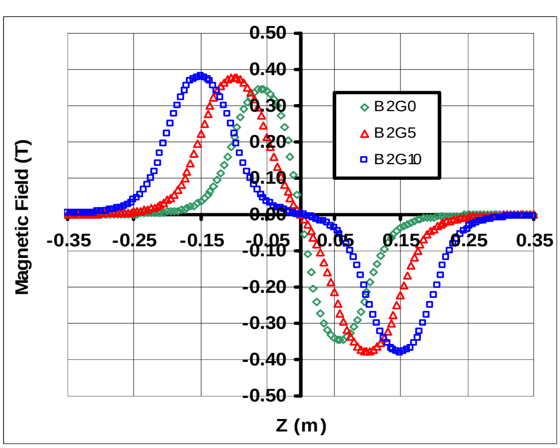

Figure 2b: Magnetic field B2 calculated for gap G=0, 5 and 10cm.

BEAM OPTICAL FEATURES

When a beam of magnetic rigidity B_ρ is launched para-axially through a GSL with a field distribution B(z) from the field free (low field) region, the general expression for focal length, f_m and beam rotation, θ are given by eqs. (5) and (6) respectively deduced from the equation of motion. The field free region for the integration limit can be approximated to the low field region fixed without any adverse effect up to the region z=-3S to +3S.

$$\frac{1}{f_p} = \frac{1}{4B\rho^2}\int_{-\infty}^{\infty} B(z)^2 dz \tag{5}$$

$$\theta = \frac{1}{2B\rho}\int_{-\infty}^{\infty} B(z)dz + \theta_0 \tag{6}$$

The field formulae B3(z) gives the exact Glaser type of bell-shaped field and was used to obtain expressions for principal focal length (fp) and principal plane location (zp) as given in eqs. (7) and (8) respectively. The mid-focal length of the lens is found as zm=fp+zp, which is given by eq. (8) also if the factor 2 is replaced by 1 on the RHS.

$$\frac{1}{f_a} = \frac{1}{a}\sin\left(\frac{\pi}{\sqrt{K^2+1}}\right) \tag{7}$$

$$\frac{1}{z_p} = \frac{-1}{a}\tan\left(\frac{\pi}{2\sqrt{K^2+1}}\right) \tag{8}$$

Where $K=(B_0 a)/(2B_\rho)$ and B_0 is the peak magnetic field at the centre of a particular GSL. These parameters should be adjusted repeatedly to achieve appropriate design of the lens after confirmation of B_0 and 'a' by numerical evaluation of the field by some standard code for the same geometry and MMF. An expression for f_p in this case is obtained by direct integration of eq. (5) using field in eq. (3) and found to be $f_a=(2a)/(K^2\pi)$, which is also found by approximating eq. (7). This gives very crude value of focal length as the lens is not weak and there is a significant change in the distance of particle from the axis inside the lens [3, p. 270]. The focal length of a MEL having GSL and anti-solenoid is estimated using the optical lens relation, $1/f_p=1/f_1+1/f_2-(2G+S)/(f_1 x f_2)$.

A particle of Bρ=0.06 T-m is projected at r=5, 3 and 1cm parallel to the central axis at different conditions G=0, 10 and 20 cm. Motion of the particle is tracked using the same matrix method for the thin lens as described in reference [2]. The crossing point of the particle track with the z-axis gives the approximate point of focus which help in finding the principal focal length f_p, mid-focal length z_m and the position of the principal plane z_p according to the above equations.

The trajectory represented by G0 and G10 curves in Fig. 3 correspond to G=0 and 10 cm. The initial values of the distance and angle of the particle are r=3 cm and r'=0 mrad respectively. As the gap G increases the focal point moves towards the origin. The combined lens become stronger with a limit when G is increased keeping other parameters constant. The net beam rotation of the beam depends on G, S and NI of individual solenoid but it is zero and independent of the gap G for overall solenoid system forming the MEL.

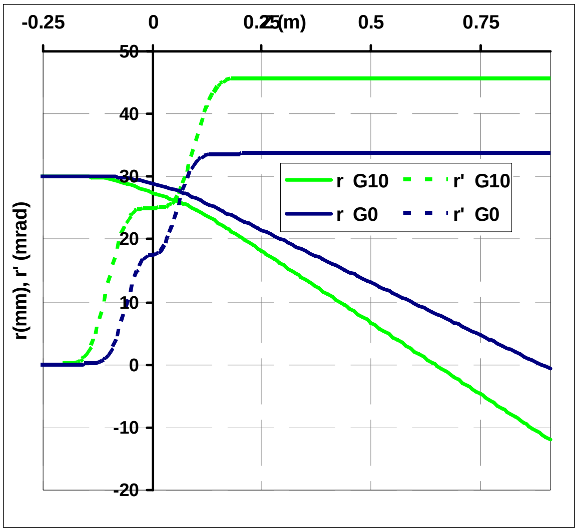

Figure 3: The distance r and angle r’ of the particle are given by solid and dotted lines at different gap G=0 cm and 10 cm respectively.

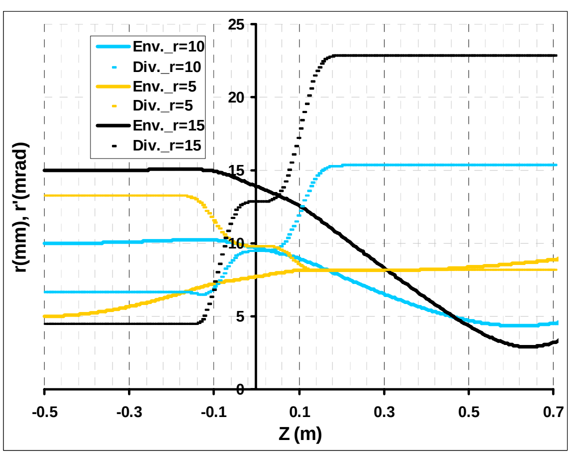

Figure 4: The beam envelops (Env.) and divergence (Div.) with initial beam width 2r and angular width 2r’ of the beam of phase space area taken to be = rr’=200 mm-mrad passing through the MEL for G=5 cm gap.

$$\sigma_f = \prod_1^f M_i \sigma_i M_i^T \qquad (9)$$

Where M is the combined transport matrix of the i-th weak lens and a drift space in between the thin lenses and σ_i is the beam matrix at the i-th weak lens in the section model. Since the initial beam is assumed to be round, the transport of the beam is represented by a 2x2 matrix multiplication appropriately. Beam transport calculation is done in usual manner employing eq. (9).

For the upright initial beam of width 20 mm and 30 mm, it is seen that the beam waist occurs at ~62 cm from the origin and it gives proper focusing to the beam as the initial beam accounts to be almost parallel with a little divergence, which is calculated from the 200/π mm-mrad beam emittance. The beam depicted in black (dark) and blue (light) colour curves in Fig. 4 show this feature of the lens. The curves of beam envelopes and beam divergences are represented by smooth line and ‘-’ marker respectively. But as we move towards the initial point object beam, the width goes on increasing while the divergence gradually decreasing. A beam with initial size of 10mm swells in size inside the lens as depicted in golden (lighter) curves in Fig. 4. This property of the lens can be used to properly control the divergence of the incoming beam by the lens to let pass through a small bore charge analyzing dipole system successfully by controlling the beam loss. The numerical values of analytical focal length (f_a), principal focal length (f_p), mid-focal length (z_m) and principal plane position (z_p) of the lens and the total beam rotation (θ) are listed for gap G, 0 , 5 and 10 cm, S and D, 10 cm and NI, 37000 A-turn in table 1 below.

Table 1: The cardinal points of the MEL using the calculated field above for different gaps G

G(cm)	f_a(cm)	f_p(cm)	z_m(cm)	z_p(cm)	θ(deg.)
0.0	85.3	89.3	89.0	-0.30	0.0
5.0	59.2	65.7	64.7	-1.0	0.0
10.0	57.7	67.3	65.0	-2.3	0.0

CONCLUSIONS

It describes the procedure of setting the MEL parameters for certain focusing power of the lens for certain beam rigidity. Since the overall rotation of the beam is zero, it curtails the effect of lens aberrations on the beam, which will be studied further in detail. The optical features were also studied to evaluate the focal length, principal plane and the beam envelop of a beam of certain phase space area. It is hoped that the study will prove to be beneficial for designing MEL for low energy beam focusing and transport more efficiently and easily.

REFERENCES

[1] N. Baba and K. Kanaya, J. Phys. E: Instrum. Vol. 12 (1979) p.525.

[2] M.H. Rashid et al., Proc. DAE-BRNS Indian Particle Accel. Conf. at RRCAT, Indore, India, InPAC-2009, Manuscript No. 115, Feb. 2009.

[3] A.B. Elkareh and J.C.J Elkareh, “Electron Beam Lenses and Optics”, Vol. 1, Academic Press, London, 1970.

[4] M. Szilagyi, “Electron Ion Optics”, Plenum Press, 1988, p. 84; G.H. Gillespie and T.A. Brown, 5th Intl. Conf. on Charged Particle Optics, Deft, The Netherlands, 1998.

[5] C. Fert and P. Durandeau, “Focusing of Charged Particles- Vol. 1”, Ed. A. Septier, Academic Press, 1967, ch. 2.3.